

² Temperature dependence of exchange biased multiferroic ³ BiFeO₃/Ni₈₁Fe₁₉ polycrystalline bilayer

⁴ J. Richy,^{1,2} T. Hauguel,¹ J. Ph. Jay,¹ S. P. Pogossian,¹ B. Warot-Fonrose,³ C. J. Sheppard,² J. L. Snyman,² A.
⁵ M. Strydom,² J. Ben Youssef,¹ A. R. E. Prinsloo,² D. Spenato,¹ and D. T. Dekadjevi^{1, a)}

¹⁾ Laboratoire de Magnétisme de Bretagne, Department of Physics, CNRS-UBO, 29285 Brest Cedex 3,
²⁾ France

²⁾ Department of Physics, University of Johannesburg, PO Box 524, Auckland Park, Johannesburg 2006,
³⁾ South Africa

³⁾ CEMES CNRS-UPR 8011, Université de Toulouse, 31055 Toulouse, France

(Dated: 15 September 2016)

The temperature dependence of exchange bias properties are studied in polycrystalline BiFeO₃/Ni₈₁Fe₁₉ bilayers, for different BiFeO₃ thicknesses. Using a field cooling protocol, a non-monotonic behavior of the exchange bias field is shown in the exchange-biased bilayers. Another thermal protocol, the Soeya protocol, related to the BiFeO₃ thermal activation energies was carried out and reveals a two-step evolution of the exchange bias field. The results of these two different protocols are similar to the ones obtained for measurements previously reported on epitaxial BiFeO₃, indicating a driving mechanism independent of the long-range crystalline arrangement (i.e., epitaxial or polycrystalline). An intrinsic property of BiFeO₃ is proposed as being the driving mechanism for the thermal dependent magnetization reversal: the canting of the BiFeO₃ spins leading to a biquadratic contribution to the exchange coupling. The temperature dependence of the magnetization reversal angular behavior agrees with the presence of such a biquadratic contribution for exchange biased bilayers studied here.

Keywords: BiFeO₃, exchange bias, angular, polycrystalline, temperature dependence

¹³ I. INTRODUCTION

¹⁴ Electrical control of magnetic nanostructures would
¹⁵ create a new generation of electronic devices directly in-
¹⁶ tegramble in actual device architecture.¹ A great deal of
¹⁷ research has been focused on an efficient way to con-
¹⁸ trol magnetic properties using an electric field, with no
¹⁹ need of an applied magnetic field.^{2–4} This research is of
²⁰ importance in the field of applied physics when consid-
²¹ ering magnetic memories or high frequency devices.^{5–7}
²² For example, spin polarized current is an effective mech-
²³ anism to transfer a torque to magnetization. However,
²⁴ it requires large current densities, leading to energy loss
²⁵ because of Joule heating effects.¹ Among the different
²⁶ possibilities of utilizing an electric control of magnetic
²⁷ properties, the use of single-phase magnetoelectric mul-
²⁸ tiferroics (MMF) is considered, as these allow a direct
²⁹ means of controlling magnetization via an electric field
³⁰ in a single heterostructure.^{7–10} Room temperature MMF
³¹ materials are rare. Among these, BiFeO₃ (BFO) is one
³² of the most studied because of its high ferroelectric (FE)
³³ polarization, with a FE Curie temperature in the order
³⁴ of 1100 K.^{11,12} In addition, the BFO possesses an an-
³⁵ tiferromagnetic (AF) order with a Néel temperature of
³⁶ about 640 K.¹³ In order to use an AF magnetoelectric
³⁷ material with no net magnetization, a ferromagnetic/AF
³⁸ exchange coupling is proposed. Meiklejohn and Bean¹⁴

³⁹ found it can be introduced by placing the AF layer in con-
⁴⁰ tact with the ferromagnetic (F) material, and is referred
⁴¹ to as exchange bias coupling. It produces an additional
⁴² anisotropy that stabilize the F layer. The existence of
⁴³ exchange bias coupling is revealed by a field shift H_e of
⁴⁴ the hysteresis cycle, named *exchange bias* field, and by a
⁴⁵ coercive enhancement. In exchange biased (EB) systems,
⁴⁶ H_e originates from the interfacial pinned spins, that is,
⁴⁷ the non-reversible part of interfacial spins. The H_c en-
⁴⁸ hancement originates in the reversible process driven by
⁴⁹ the AF anisotropy. This anisotropy provides additional
⁵⁰ critical fields that will hinder the domain wall motion in
⁵¹ the F layer.^{15,16} In recent years many research projects
⁵² have been undertaken to understand the exchange bias
⁵³ coupling in BFO/F nanostructures.^{17–21} However, there
⁵⁴ is still no clear understanding of the origins of this cou-
⁵⁵ pling.

⁵⁶ Among the properties of interest, the thermal depen-
⁵⁷ dence of magnetization reversal is a key phenomenon
⁵⁸ that need to be understood in AF/F systems due to its
⁵⁹ relevance for applied issues in magnetic recording, and
⁶⁰ for fundamental issues related to the thermodynamics of
⁶¹ nanoscale magnetic systems. Effectively, understanding
⁶² and tailoring the thermal dependence of the magnetiza-
⁶³ tion reversal is of interest for applied issues, as this de-
⁶⁴ pendence can be inferred by laser heating²² or applied
⁶⁵ current.²³ In addition, it should be considered that a de-
⁶⁶ vice can be compromised by temperature fluctuations in
⁶⁷ a magnetic field.²⁴ Consequently, considering the partic-
⁶⁸ ular interest of BFO/F systems, the thermal dependence

^{a)}david.dekadjevi@univ-brest.fr

69 of the BFO/F magnetization reversal needs to be un-
 70 derstood. Previous experimental studies on BFO/F sys-
 71 tems have revealed an intriguing non-monotonic evolu-
 72 tion of the exchange bias field with temperature T .^{25–28}
 73 Furthermore, this phenomenon is found in epitaxial^{25–27}
 74 and polycrystalline²⁸ bilayers, for different F (including
 75 CoFe, CoFeB, Co and NiFe) coupled with BFO, and for
 76 different BFO thicknesses. This common phenomenon
 77 in BFO/F systems is not yet understood despite its key
 78 importance.

79 In the research work presented here, the thermal be-
 80 havior of polycrystalline BiFeO₃/Ni₈₁Fe₁₉ is studied for
 81 different BFO thicknesses (t_{BFO}), using complementary
 82 approaches. Results are analyzed considering previous
 83 findings on the thermal magnetization reversals of not
 84 only polycrystalline but also epitaxial BFO/F systems,
 85 so as to gain a better understanding of the origin of the
 86 non-monotonic evolution of the exchange bias field with
 87 temperature.

88 In the first section of this manuscript experimental pro-
 89 cedures are described. In the second section, a struc-
 90 tural study analysis involving transmission electron mi-
 91 croscopy (TEM) and two dimensional (2D) temperature
 92 dependent X-ray diffraction (XRD) is provided. This was
 93 used to probe the crystallographic and the morphologic
 94 properties of the BFO/F bilayers. In the third section,
 95 the thermal dependence of magnetization reversals, in-
 96 cluding exchange bias and coercive fields evolutions, are
 97 studied using a field-cooled protocol in order to probe
 98 the presence of a non-monotonic behavior in the sam-
 99 ples. In the fourth section, the exchange bias field evo-
 100 lution following a specific protocol, called here the Soeya
 101 protocol,²⁹ is showed. This protocol, initially proposed
 102 by Soeya *et al.*,²⁹ and later modified by O’Grady *et al.*,³⁰
 103 was used to probe the thermal activated energies of all
 104 BFO/F samples in this study. It should be noted that
 105 this paper is the first study to investigate this thermal
 106 dependent protocol in polycrystalline exchange-biased
 107 BFO/F samples. Finally, the thermal dependence of
 108 the magnetization reversal angular evolution is probed,
 109 as this will provide information on the various effective
 110 anisotropies of exchange-bias systems.

111 II. EXPERIMENTAL PROCEDURES

112 The heterostructures BiFeO₃/Ni₈₁Fe₁₉ (BFO/Py)
 113 were grown by radio frequency sputtering, sequentially
 114 deposited using the structure Pt(30 nm)/BFO(t_{BFO})/
 115 Py(10 nm)/Pt(30 nm) on a naturally oxidized silicon sub-
 116 strate. An in-plane deposition field $H_{\text{dep}} = 30 \text{ mT}$ mag-
 117 netic field was applied during the growth process. Fur-
 118 ther details on the growth process are available in previ-
 119 ous publications.^{31,32} The BFO nominal thicknesses were
 120 equal to 0 nm, 29 nm and 177 nm, further referred to as
 121 sample S₀, S₂₉ and S₁₇₇. The BFO critical thickness t_c
 122 above which H_e is not zero, was determined earlier to
 123 be 23 nm in the BFO/Py system presented here.³² Thus,

124 these samples are representative of three different thick-
 125 ness intervals of $H_e(t_{\text{BFO}})$: i) S₀ corresponds to an un-
 126 biased sample; ii) S₂₉ with $t_{\text{BFO}} = 29 \text{ nm}$ is just above
 127 t_c , an interval where $H_e(t_{\text{BFO}})$ is strongly thickness de-
 128 pendent; and iii) S₁₇₇ with $t_{\text{BFO}} = 177 \text{ nm}$ is far
 129 larger than t_c , an interval where $H_e(t_{\text{BFO}})$ is thickness
 130 independent.

131 In order to characterize the samples’ structural prop-
 132 erties, TEM and XRD measurements were carried out.
 133 TEM analyses on the samples were done using a TEC-
 134 NAI F-20 system operating at 200 kV, equipped with a
 135 spherical aberration corrector for the objective lens in or-
 136 der to avoid the delocalization effect at interfaces. The
 137 crystallographic properties of the samples were probed
 138 by XRD, using a 2D Oxford diffractometer (X-Calibur-2
 139 model) in the temperature range from 100 K to 300 K.

140 Temperature dependent magnetic measurements were
 141 initially performed using a superconductive quantum in-
 142 terference device (SQUID) magnetometry. In order to
 143 correct the data for remnant fields that might exist in the
 144 SQUID magnet, care was taken during the measurement
 145 protocols to correct for this. Two different measurement
 146 protocols were performed using the SQUID. These two
 147 protocols were i) the field cooled (FC) protocol, and ii)
 148 the Soeya protocol,²⁹ that will be discussed in detail later
 149 in the text.

150 In the FC protocol, the samples were cooled from 300 K
 151 to 10 K, in a $\mu_0 H_{\text{FC}} = 100 \text{ mT}$ field along the H_{dep} direc-
 152 tion. In order to dispose of all possible training effects,
 153 four field-switchings were performed at 10 K between
 154 negative and positive H_{FC} . The magnetic hysteresis (M-
 155 H) loops were then recorded at different temperatures
 156 between 10 K to 380 K, in increasing temperature steps.

157 In the Soeya protocol, the samples were heated un-
 158 der a positive magnetic field H_{FC} applied along H_{dep}
 159 at a preset temperature $T_{\text{set}} = 380 \text{ K}$, and subsequently
 160 cooled under the same H_{FC} down to a measurement tem-
 161 perature $T_m = 10 \text{ K}$. Then, after reversing the field to
 162 $-H_{\text{FC}}$, the system was annealed at an intermediate ac-
 163 tivation temperature T_a , leading to the reversal of AF
 164 entities with low energy compared to the thermal energy
 165 at T_a . Finally, returning to T_m , an M-H loop was mea-
 166 sured. This process was repeated for different T_a values.
 167 In the Soeya protocol, $H_e(T_a)$ depends on the thermal
 168 activation energies present in the magnetic system. In-
 169 deed, above a given temperature defined as a blocking

170 temperature, an energy barrier in the AF is overcome
 171 by the thermal agitation. In a AF/F system, different
 172 kinds of energy barriers can be expected to exist, such
 173 as: i) anisotropy energy barriers related to grain sizes or
 174 magnetic domain sizes, ii) domain wall nucleation and
 175 depinning energies, and iii) magnetic coupling energies
 176 (including complex interfacial couplings such as a spin-
 177 glass like coupling). Consequently, a distribution of the
 178 blocking temperatures can arise as a consequence of dif-
 179 ferent phenomena involved. In principle, the evolution of
 180 $H_e(T_a)$ may be attributed to any of the fore-mentioned
 181 energy barriers in EB systems.^{30,33–35}

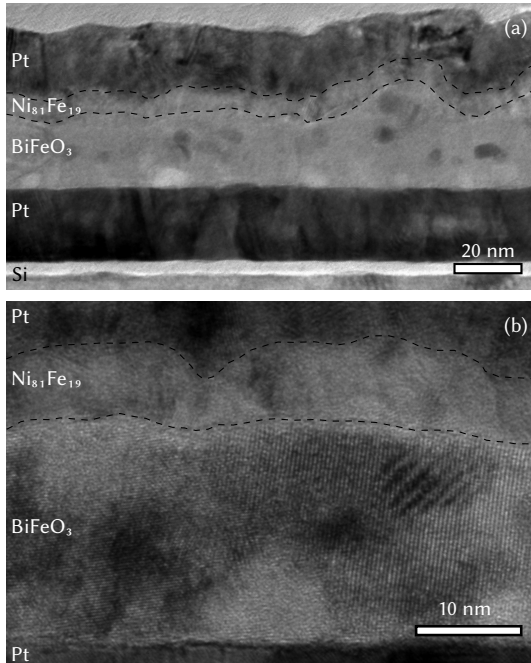


FIG. 1. Cross-section transmission electron micrography of the S₂₉ sample. Dashed lines are guides to the eye, and delimit the Py layer.

In order to probe the temperature dependent anisotropy configuration, M-H loops were measured for different applied field directions φ , where φ is the azimuthal angle with respect to H_{dep} , using a custom made vibrating sample magnetometer (VSM). These measurements were done at room temperature (RT) and 77 K. In order to perform the 77 K measurements, the samples were immersed in liquid nitrogen.

III. RESULTS AND DISCUSSIONS

A. Structural properties

In Fig. 1 the TEM image of the S₂₉ sample cross-section is shown. It can be seen from Fig. 1 that the various layers are well defined within the film layer stack. The surface roughness of the Py layer is due to the surface roughness of the BFO. TEM analysis of the S₁₇₇ sample shows an increase in the roughness of the Py layer when compared to that observed in S₂₉, confirming an increase in the surface roughness with the increase of t_{BFO} , previously observed using atomic force microscopy measurements for $t_{\text{BFO}} > 23$ nm on this BFO/Py system.³² In order to investigate the BFO crystalline arrangement and its evolution with temperature, 2D XRD patterns were obtained on sample S₁₇₇ at 50 K intervals in the temperature range from 100 K to 296 K. Examples of these XRD patterns are shown in Fig. 2. It revealed

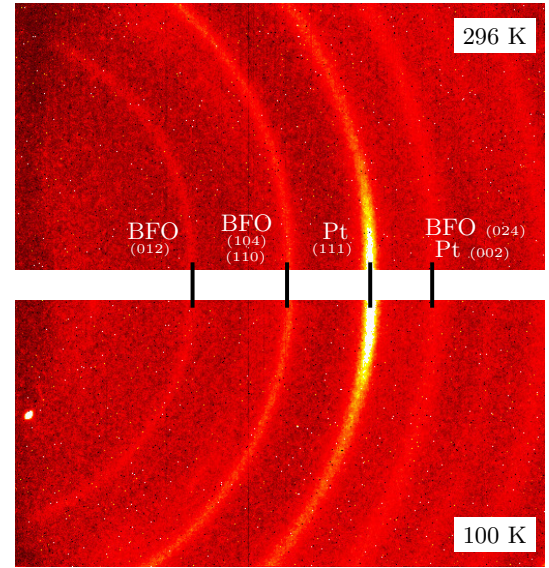


FIG. 2. XRD patterns at two different temperatures for the S₁₇₇ heterostructure. The circular rings show the BFO polycrystallinity, and the non-uniform (111) Pt diffraction ring reveals a preferred growth direction for the Pt layer.

intensity of the rings for the Pt layer. This is due to the preferred (111) growth direction of the Pt layer. There was no temperature dependence in these XRD diagrams, indicating the temperature stability of the BFO crystallographic arrangement.

B. Temperature dependent magnetization reversal using the FC protocol

In Fig. 3 the M-H measurements using the FC protocol are shown for (a) S₀, (b) S₂₉ and (c) S₁₇₇. From figures 3(b) and 3(c) it is seen that for samples S₂₉ and S₁₇₇, the M-H loops are shifted along the field axis. In addition, coercive field enhancements are observed for S₂₉ and S₁₇₇ compared to the values found for S₀ at the same temperature. The presence of the exchange bias and the coercive enhancement are characteristics of EB systems.³⁶ It should be noted that the significant roughness observed in S₂₉ and S₁₇₇ could also contribute to the coercivity enhancement.³⁷

The behavior of $H_c(T)$ and $H_e(T)$ are extracted from the FC protocol M-H measurements for all the samples and are shown in Fig. 4. The coercive field H_c decreases monotonically with increasing temperature for all the samples, as is typically expected in F materials and EB systems. This behavior therefore corresponds to previously reported experimental studies on polycrystalline and epitaxial BFO/F exchange biased systems.^{25–28,38}

In Fig. 4(b) the $H_e(T)$ behavior of the various samples are shown. It is clear from the figure that H_e is zero and does not vary with temperature for the unbiased S₀ sample. The $H_e(T)$ behavior of the S₂₉ and S₁₇₇

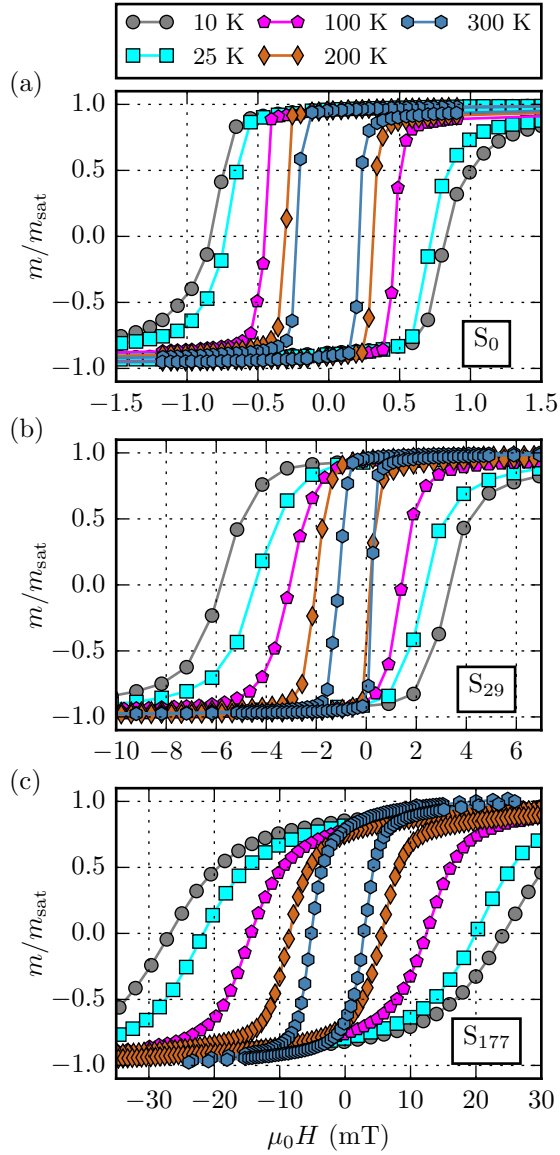


FIG. 3. Hysteresis cycles at different temperatures indicated, following the FC protocol for (a) S₀, (b) S₂₉ and (c) S₁₇₇ samples. Note the different x -axis scales.

samples does not show a monotonic decrease, but exhibits a sharp decrease at low temperature, displaying a peak at an intermediate temperature. In the present study this peak appears at 175 K for S₂₉, and at 250 K for S₁₇₇, respectively. This non-monotonic $H_e(T)$ behavior is a common behavior for BFO bilayers, in the sense that it is relevant to different F coupled to BFO.^{25–28} This behavior is also common in both polycrystalline²⁸ and epitaxial BFO.^{25–27} Thus, the driving mechanism for a non-monotonic $H_e(T)$ behavior of BFO/F should not depend on the BFO crystallographic arrangement, nor t_{BFO} or the thickness and composition of the F layer.

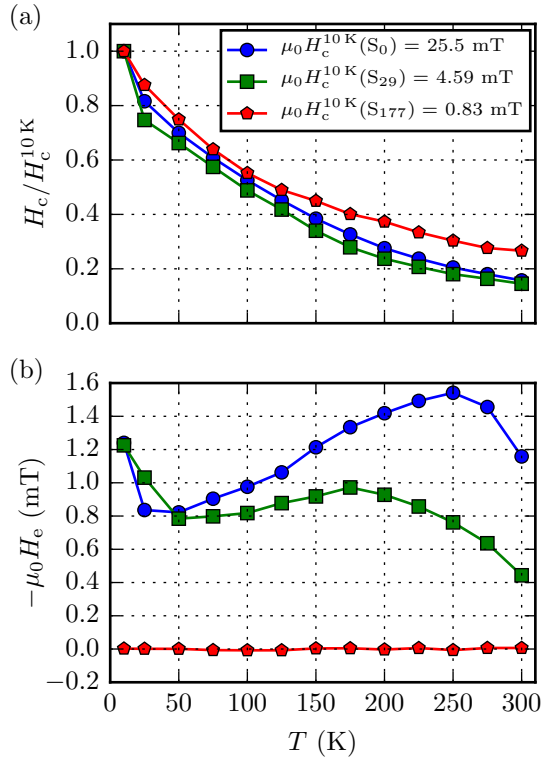


FIG. 4. Temperature evolution following the FC protocol of (a) the reduced coercive field $H_c/H_c^{10\text{K}}$ and (b) the exchange field H_e , for S₀ (red pentagon), S₂₉ (green squares) and S₁₇₇ (blue circles) samples. The $\mu_0 H_c$ values at 10 K for the three samples are indicated in the legend of figure (a).

251 C. Temperature dependent magnetization reversal using the 252 Soeya protocol

253 As the thermal evolution of H_e depends on thermal
254 evolutions of the AF entities which are pinned, it is of
255 interest to probe the BFO thermal activation energies
256 present in our samples. In order to investigate the ther-
257 mal behavior, the Soeya protocol was used. It may be
258 noted that while the Soeya protocol has been performed
259 on epitaxial exchange coupled BFO,³⁴ it has, however,
260 never before been performed on polycrystalline exchange
261 coupled BFO.

262 The S₂₉ and S₁₇₇ hysteresis loops obtained from the
263 Soeya protocol in the temperature range of 10 K to 380 K
264 are shown in Fig. 5. The $H_e(T_a)$ and $H_c(T_a)$ curves were
265 extracted from these hysteresis loops and are reported
266 in Fig. 6. For both samples, $H_c(T_a)$ is constant (not
267 shown), as all the experiments were performed at the
268 same T_m . However, Fig. 6 indicates that H_e evolves with
269 the activation temperature T_a . $H_e(T_a)$ of both S₂₉ and
270 S₁₇₇ exhibit similar two-step like behavior: i) the first
271 step is seen before 100 K, ii) while second step is seen
272 above 250 K. For both steps, H_e presents a significant
273 variation with T_a . In between these two steps, $H_e(T_a)$ for

S₂₉ and S₁₇₇ are different: in S₂₉, it exhibits a positive slope with increasing T , whereas for S₁₇₇, it is constant. A two-step $H_e(T_a)$ evolution in the Soeya protocol was previously reported for BFO/CoFeB epitaxial system.³⁴ This two-step reversal was attributed to two different contributions: at low temperature, the AF/F disordered interfacial spins would exhibit a spin-glass like behavior and would then be responsible for the first step of $H_e(T_a)$, whereas domain wall depinning energy would be the driving mechanism for the second step. The behavior observed in Fig. 6 are similar than those observed for epitaxially grown BFO/CoFeB, where t_{BFO} were chosen to be in the same thickness intervals.³⁴ The only difference between the present values of H_e and those observed in epitaxially grown BFO is the magnitude of H_e . This is expected as the H_e magnitude is related to the F thickness and magnetization, which were different in these studies. Thus, this common evolution of H_e with T_a indicates a driving mechanism independent of the long-range crystalline arrangement (i.e., epitaxial or polycrystalline arrangement) and of the nature of the F layer. Indeed, it is rather unlikely that two distinct mechanisms, the first one present in polycrystalline films and the second one present in epitaxial ones, would result in exactly the same $H_e(T_a)$ behavior. This is even more unlikely for two different t_{BFO} intervals. If truly present, the driving mechanism proposed for the epitaxial BFO, involving spin-glass like interfacial disorder and domain wall depinning energy, should be valid for the polycrystalline samples. However, it is not expected that the domain wall depinning energy would be the same in polycrystalline and epitaxial systems: such an energy would certainly depend on the crystalline arrangement. Consequently, it is of interest to analyze this common $H_e(T_a)$ two-step behavior in BFO, and the common non-monotonic $H_e(T)$ behavior considering that both phenomena are driven by a BFO physical property independent of its long-range crystalline arrangement.

An inherent BFO property that can be considered is the canting of the BFO spins. This canting is present in either polycrystalline BFO or epitaxial BFO.^{39–44} Such a canting results in a non-zero component of the BFO magnetic moment, oriented in a perpendicular direction compared to the non-canted case. Consequently, in a BFO/F bilayer, the exchange coupling energy resulting from this non-zero component will be a minimum in the perpendicular direction. This phenomenon is similar to the one proposed by Slonczewski to describe perpendicular exchange coupling in Fe/Cr multilayers,⁴⁵ involving a biquadratic exchange energy term. Furthermore, previous micromagnetic calculations confirmed that perpendicular coupling does result when canting is allowed.⁴⁶

In the BFO/F systems discussed here, the biquadratic coupling promoted by intrinsic BFO properties such as the canted spins should contribute to the exchange bias properties. Indeed, it was recently shown by simulation that the presence of biquadratic coupling in AF/F systems results in a non-monotonic behavior of $H_e(T)$, with

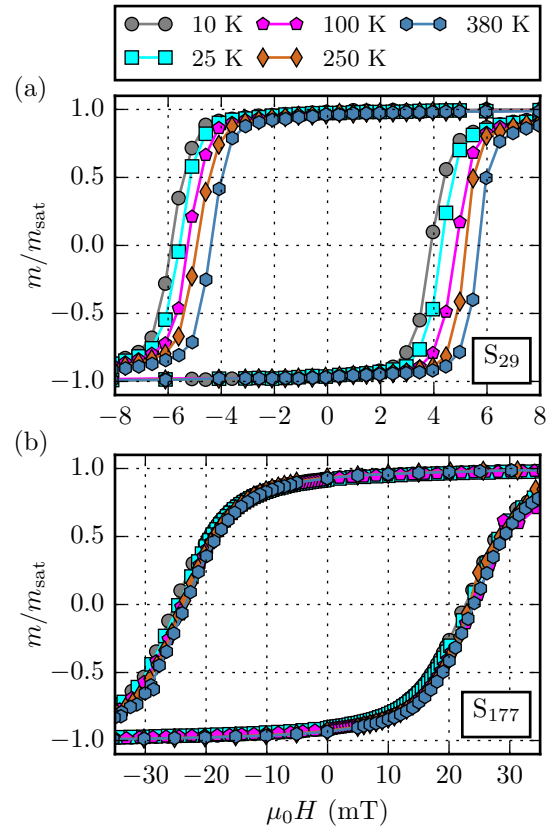


FIG. 5. Hystereris cycles at different temperatures using the Soeya protocol for (a) S₂₉, and (b) S₁₇₇ samples.

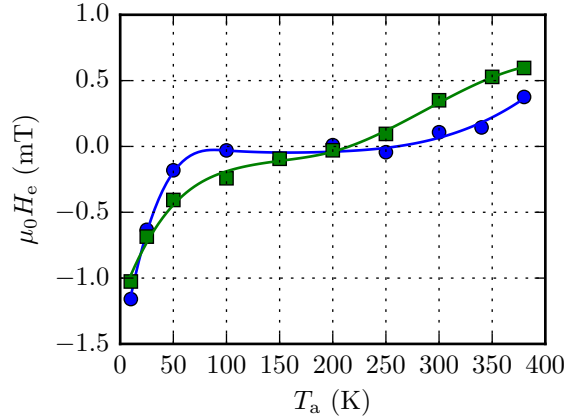


FIG. 6. Evolution of H_e using the Soeya protocol for S₂₉ (green squares) and S₁₇₇ (blue circles) samples.

the presence of a peak at intermediate temperature.⁴⁷ This supports the idea of a driving mechanism relying on an inherent BFO property, that is, the presence of canted spins being at the origin of the common temperature dependent phenomenon observed in epitaxial and polycrystalline BFO/F systems. To probe the presence

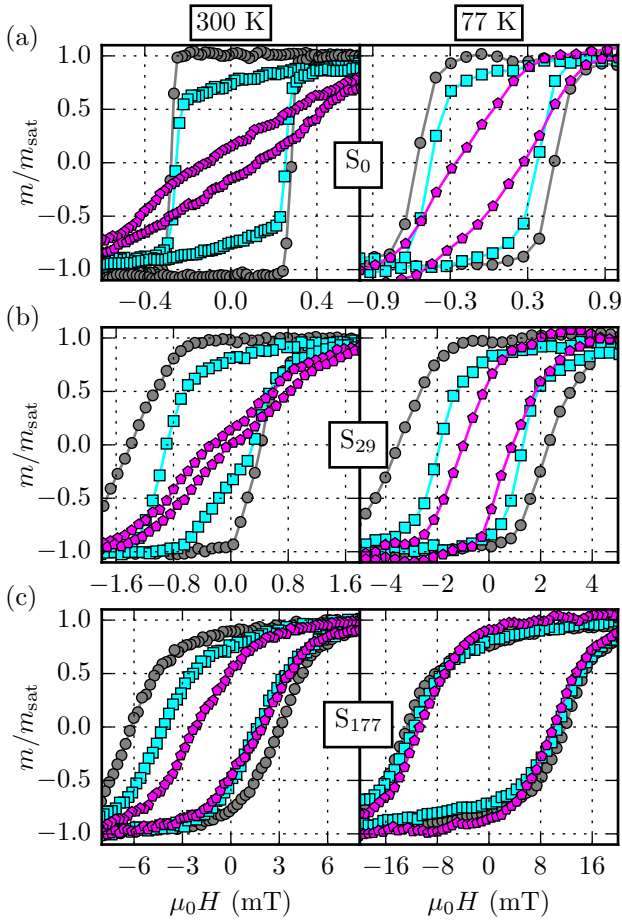


FIG. 7. Magnetization versus field curves obtained using the VSM for $T = 300 \text{ K}$ (left) and $T = 77 \text{ K}$ (right), for various thicknesses t_{BFO} (a) 0 nm, (b) 29 nm and (c) 177 nm. Measurements were performed with field angles at 0° (gray circles), 45° (cyan squares) and 90° (magenta pentagons) away from the uniaxial easy anisotropy axis (i.e. $\varphi \approx 20^\circ$ for S_0 , $\varphi \approx 10^\circ$ for S_{29} and $\varphi = 0^\circ$ for S_{177}).

338 of a biquadratic coupling in the samples studied here,
339 the angular dependence of the magnetization reversal was
340 measured using VSM measurements at RT and at 77 K.

341 D. Temperature dependent magnetization reversal using 342 azimuthal measurements

343 Magnetization reversal loops were measured at 77 K
344 and RT, applying the external field H at various φ angles.
345 Results are shown in Fig. 7. $H_c(\varphi)$ and $H_e(\varphi)$ obtained
346 from the measurements in Fig. 7 are shown in Fig. 8
347 and Fig. 9, respectively. For all samples and at both
348 temperatures, M-H behaviors are shown to be strongly
349 dependent on the thickness of BFO.

350 In Fig. 8 the H_c angular dependence is shown for the
351 sample in which BFO was absent (S_0), for both measure-
352 ments at RT and 77 K. $H_c(\varphi)$ exhibits a maximum at

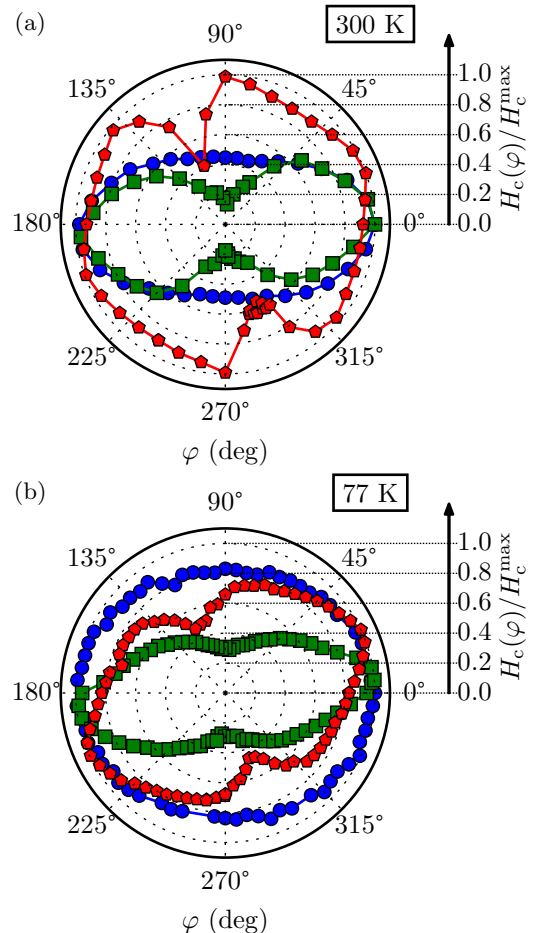


FIG. 8. Azimuthal evolution of the reduced coercive field $H_c(\varphi)/H_c^{\text{max}}$ at (a) 300 K and (b) 77 K, with $t_{\text{BFO}} = 0 \text{ nm}$ (red pentagons), 29 nm (green squares) and 177 nm (blue circles).

353 $\varphi = 20^\circ$ and a minimum at $\varphi = 110^\circ$ shown in Fig. 8(a)
354 at 300 K. This confirms the uniaxial character of the non-
355 coupled $\text{Ni}_{81}\text{Fe}_{19}$ layer anisotropy. The reversals at
356 $\varphi = 20^\circ$ and $\varphi = 110^\circ$ are typical of an uniaxial easy axis
357 loop for $\varphi = 20^\circ$ and hard axis for $\varphi = 110^\circ$, as shown
358 in Fig. 7(a). The hysteresis observed along the hard axis
359 implies an angular dispersion of the easy axis. Thus, Py
360 is uniaxial with a 20° misaligned easy axis relatively to
361 H_{dep} . This analysis is valid for both temperatures.

362 The Py layer coupled with a thin BFO layer in the
363 S_{29} sample exhibits a coercive enhancement (at 300 K)
364 compared to S_0 , and an angular dependent shift of the
365 hysteresis loop along the field axis as shown in Fig. 8(a)
366 and in Fig. 9(a), respectively. The H_c angular depen-
367 dence exhibit a maximum at $\varphi = 5^\circ$ and a minimum
368 at $\varphi = 95^\circ$ as shown in Fig. 8(a). At 300 K, a two-
369 step magnetization reversal process is observed when H
370 is at 95° (i.e., along the H_c minimum). Such a two-
371 step reversal reveals a minimum of the magnetic energy
372 along that direction, as expected from the contribution
373 of a biquadratic coupling term which favors a perpen-

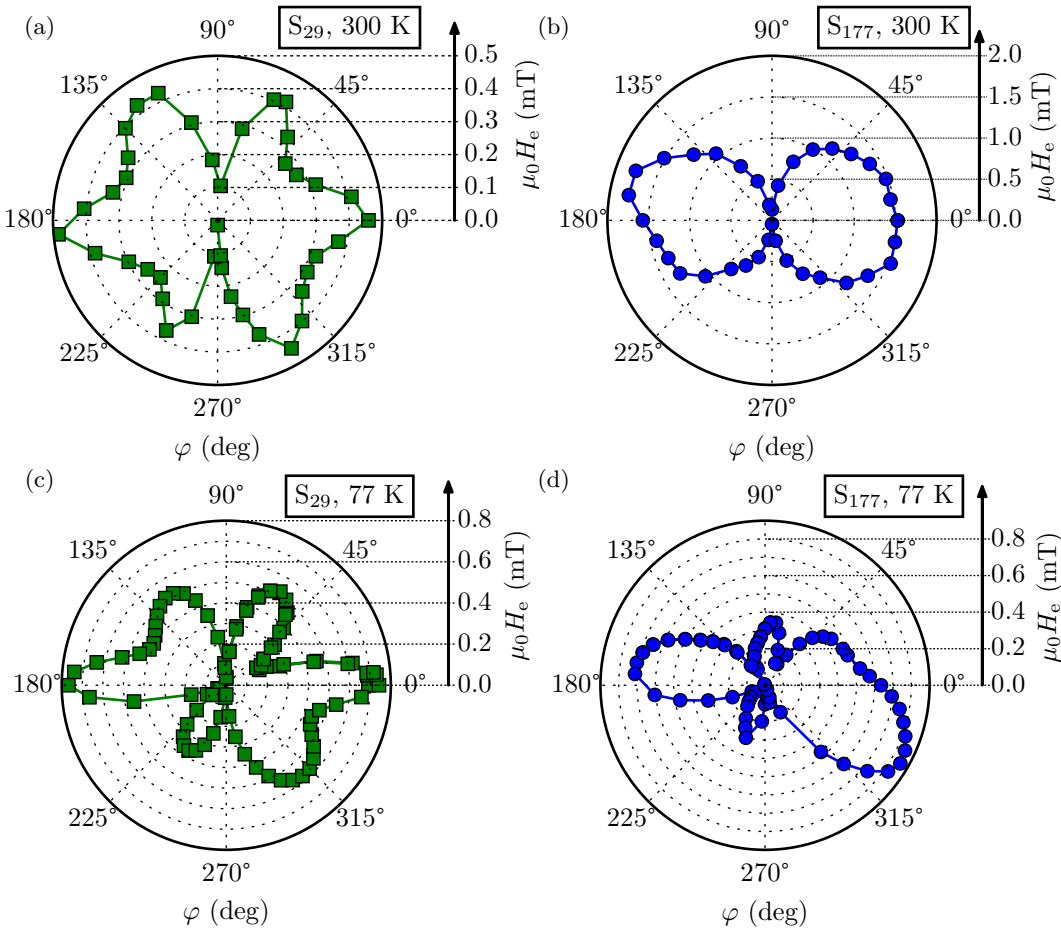


FIG. 9. Angular evolution of H_e : (a) and (b), at 300 K; (c) and (d), at 77 K. The samples measured are S₂₉ (green squares) and S₁₇₇ (blue circles).

374 dicular orientation of the F moments relatively to the
375 AF ones.^{48–53} It reveals that the canting in BFO plays a
376 key role for the S₂₉ magnetization reversal and support
377 the hypothesis of the canting being a driving mechanism
378 for the exchange biased properties and their temperature
379 dependence. Furthermore, it should be noted that the
380 two-step magnetization reversal reported here was also
381 observed in a previous experimental study on epitaxial
382 Co₇₅Fe₂₅/BFO and Co₅₀Fe₅₀/BFO.²⁶ However, this fea-
383 ture was not discussed by the authors. In this previous
384 work, $H_e(T)$ exhibited a similar non-monotonic behavior
385 to the one reported here in Fig. 4(b).

386 It should be noted that the exchange coupling of the
387 Py with the thin BFO layer does not modify the over-
388 all shape of the $H_c(S_{29})$ angular dependence (relatively
389 to the uncoupled Py in S₀), despite the biquadratic con-
390 tribution. The absence of a fourfold symmetry arising
391 from a biquadratic contribution suggests that the uniax-
392 ial anisotropy energy is greater than the biquadratic con-
393 tribution to the magnetic anisotropy energy. Thus, the
394 evidence for a contribution which favors a 90° phase is the
395 two-step magnetization reversal process along the per-

396 perpendicular direction to the uniaxial easy axis,^{49–51,53} as
397 previously discussed in Fig. 7(b). This two-step magne-
398 tization reversal and the H_c angular dependence demon-
399 strate that the uniaxial anisotropy dominates the bi-
400 quadratic contribution in S₂₉. At 77 K, the overall shape
401 of the H_c angular dependence is similar but the minimum
402 observed along the uniaxial hard axis is less pronounced
403 than the one observed at 300 K as shown in Fig. 8(b).
404 It indicates that the anisotropy dispersion is more pro-
405 nounced at 77 K than at 300 K. This is confirmed by the
406 large opening of the hysteresis curves shown in Fig. 7.

407 The Py layer coupled with a thick BFO layer in the
408 S₁₇₇ sample exhibits an enhanced coercivity relatively to
409 S₀ and S₂₉, as shown in Fig. 7(c). In Fig. 8(a), the H_c
410 angular dependence of S₁₇₇ at 300 K corresponds to an
411 ellipse. There is no local minimum at 90° of the easy
412 axis, indicating a large dispersion of the anisotropy axis.
413 The angular dependence of H_c at 77 K is quasi-circular
414 revealing a random anisotropy dispersion.

415 The H_e angular dependence in exchange biased sys-
416 tems depends on the ratio of the unidirectional and
417 anisotropic energy contributions.^{54–56} At RT, the H_e an-

418 gular dependence for S₂₉ is characteristic of a misaligned 473 exchange coupled with the BFO one. This H_e and H_c
 419 configuration of the anisotropy axes. Indeed, the pres- 474 temperature behavior confirm previous experimental be-
 420 ence of a star-like azimuthal shape is well-known and can 475 haviors on epitaxial and polycrystalline BFO/F systems,
 421 be reproduced using a coherent rotation model.^{54,56} In 476 demonstrating that this H_e(T) non-monotonic behav-
 422 such a shape, the misalignment is revealed by the as- 477 ior is independent of the BFO crystalline arrangement,
 423 symmetry of the arms. Thus, as shown for S₂₉ in Fig. 9(a), 478 thickness, and independent on the F nature.
 424 the misalignment is indicated by the reduced H_e maxi- 479 The second thermal approach was carried out on the
 425 mum value at $\varphi = 65^\circ$ and $\varphi = 245^\circ$) relatively to the 480 exchange-coupled samples (i.e., S₂₉ and S₁₇₇) and con-
 426 ones at $\varphi = 120^\circ$ and $\varphi = 300^\circ$, respectively. At RT 481 sists of the Soeya protocol which relates to the BFO
 427 in Fig. 9(b), the H_e(S₁₇₇) angular dependence exhibits 482 thermal activation energies at the origin of the exchange
 428 two asymmetric lobes, relatively to the easy axis. In a 483 bias properties. The evolution of H_e with the activa-
 429 recent work, the presence of two asymmetric exchange 484 tion temperature presents a two-step evolution for both
 430 lobes in BFO/Py could be reproduced using a coherent 485 samples. This behavior in the polycrystalline BFO/Py
 431 rotation model considering a biquadratic-like anisotropy 486 system studied here is identical to the one observed in
 432 and a small 5° misalignment between the anisotropy axis 487 epitaxial BFO. Consequently, the thermal behavior of
 433 directions.³¹ For both samples, the H_e angular shape 488 the BFO/F exchange bias field probed here is shown to
 434 is strongly temperature dependent since the curves ob- 489 be independent of the crystalline arrangement, thickness,
 435 tained at 77 K are much different than the ones obtained 490 and independent on the F nature. It indicates that the
 436 at 300 K, as shown in Fig. 9. Since the H_e angular de- 491 driving mechanism for a non-monotonic H_e in exchange
 437 pendences are strongly dependent of the ratio between 492 coupled BFO systems relies on a physical property or
 438 effective anisotropy constants, this temperature depen- 493 properties not related to the ones discussed above. An in-
 439 dence is expected as H_e(T) and H_c(T) evolves in a much 494 trinsic driving property of BFO is proposed as being this
 440 different manner with temperature as shown in Fig. 9 and 495 driving mechanism: the canting of the BFO spins leading
 441 Fig. 8, indicating a much different evolution of the vari- 496 to a biquadratic contribution to the exchange coupling.
 442 ous effective anisotropies in a given sample. The thermal 497 The third thermal approach was to probe the magneti-
 443 dependent azimuthal measurements demonstrate complex 498 zation reversal angular dependencies at RT and at 77 K,
 444 arrangements of the anisotropy axis and are in agree- 499 as it provides information concerning axial and unidirec-
 445 ment with the presence of a biquadratic contribution to 500 tional properties. For sample S₂₉, the magnetization re-
 446 the magnetic energy of the BFO/Py studied here. A bi- 501 versal angular dependence demonstrates the presence of
 447 quadratic driving mechanism for the thermal properties 502 a biquadratic contribution. For all samples, the tempera-
 448 of BFO/F systems induced by the canting of the BFO 503 ture dependence of the angular behavior of the magneti-
 449 spins depends neither on the long-range crystalline ar- 504 zation reversal agrees with the presence of a biquadratic
 450 rangement of the BFO nor on the F layer, as it is an 505 contribution and is driven by the anisotropic ratio, in-
 451 intrinsic property of BFO. It is in agreement with pre- 506 cluding the presence of misalignments.
 452 viously reported H_e(T) and H_c(T) behaviors following a 507 Therefore, a common mechanism of a biquadratic con-
 453 FC protocol and the H_e(T_a) behavior following the Soeya 508 tribution, for driving temperature dependent exchange
 454 protocol, in polycrystalline and epitaxial BFO. 509 bias properties, is supported by the thermal dependent
 455 IV. CONCLUSION 510 studies presented here. It is of interest to implement ex-
 456 In the current contribution, the thermal dependences 511 plicitly such a mechanism in theoretical approaches in or-
 457 of exchange bias properties are probed for three different 512 der to predict and tailor the thermal dependent exchange
 458 BFO thicknesses (0 nm, 29 nm and 177 nm). These were 513 bias properties in BFO systems.

456 In the current contribution, the thermal dependences
 457 of exchange bias properties are probed for three different
 458 BFO thicknesses (0 nm, 29 nm and 177 nm). These were
 459 chosen as they represent three regions of interest in the
 460 magnetic behavior of the BFO/Py system: i) S₀ corre-
 461 sponds to an unbiased sample; ii) t_{BFO} = 29 nm (S₂₉)
 462 is just above t_c, an interval where H_e (t_{BFO}) is strongly
 463 thickness dependent; and iii) t_{BFO} = 177 nm (S₁₇₇) is far
 464 larger than T_C, an interval where H_e (t_{BFO}) is thickness
 465 independent. Three different methods were employed to
 466 study the thermal dependence of the exchange bias of
 467 BFO/Py system.

468 The first approach consists of a field cool procedure.
 469 It shows that H_c(T) decreases monotonically with increas-
 470 ing temperature for all BFO thicknesses, whereas H_e(T)
 471 exhibits a non-monotonic behavior, with the presence of
 472 a middle temperature range peak, when the Py layer is

514 ACKNOWLEDGMENTS

515 We acknowledge the french microscopy network
 516 METSA for TEM experiments, and the PIMM-DRX
 517 shared facility of the university of Brest for XRD mea-
 518 surements. The authors also thank R. Tweed for read-
 519 ing through the manuscript. A. R. E. Prinsloo and C.J.
 520 Sheppard thanks the FRC/URC of UJ and SA-NRF
 521 for the financial support (Protea funding: 85059). A.
 522 M. Strydom thanks the FRC/URC of UJ and the SA-
 523 NRF (93549) for financial assistance. D. T. Dekadjevi
 524 thanks the MAEDI and MENESR for the financial sup-
 525 port (PHC PROTEA 2014 N°29785ZA9).
 526 All the figures were generated using the Matplotlib
 527 software.⁵⁷

- ⁵²⁸ ¹F. Matsukura, Y. Tokura, H. Ohno, F. Matsukura, Y. Tokura, and H. Ohno, "Control of magnetism by electric fields," *Nature Nanotechnology* **10**, 209–220 (2015).
- ⁵³¹ ²D. Chiba, M. Sawicki, Y. Nishitani, Y. Nakatani, F. Matsukura, H. Ohno, F. Matsukura, Y. Tokura, and H. Ohno, "Magnetization vector manipulation by electric fields," *Nature* **455**, 515–518 (2008).
- ⁵³⁴ ³S. M. Wu, S. A. Cybart, P. Yu, M. D. Rossell, J. X. Zhang, R. Ramesh, R. C. Dynes, F. Matsukura, Y. Tokura, and H. Ohno, "Reversible electric control of exchange bias in a multiferroic field-effect device," *Nature Materials* **9**, 756–761 (2010).
- ⁵³⁹ ⁴J. T. Heron, M. Trassin, K. Ashraf, M. Gajek, Q. He, S. Y. Yang, D. E. Nikonorov, Y.-H. Chu, S. Salahuddin, and R. Ramesh, "Electric-field-induced magnetization reversal in a ferromagnet-multiferroic heterostructure," *Physical Review Letters* **107**, 217202 (2011).
- ⁵⁴⁴ ⁵Y.-H. Chu, L. W. Martin, M. B. Holcomb, M. Gajek, S.-J. Han, Q. He, N. Balke, C.-H. Yang, D. Lee, W. Hu, Q. Zhan, P.-L. Yang, A. Fraile-Rodríguez, A. Scholl, S. X. Wang, R. Ramesh, F. Matsukura, Y. Tokura, and H. Ohno, "Electric-field control of local ferromagnetism using a magnetoelectric multiferroic," *Nature Materials* **7**, 478–482 (2008).
- ⁵⁵⁰ ⁶W. Eerenstein, N. D. Mathur, and J. F. Scott, "Multiferroic and magnetoelectric materials," *Nature* **442**, 759–65 (2006).
- ⁵⁵² ⁷M. Bibes and A. Barthélémy, "Multiferroics: towards a magnetoelectric memory," *Nature materials* **7**, 425–6 (2008).
- ⁵⁵⁴ ⁸T. Zhao, A. Scholl, F. Zavaliche, K. Lee, M. Barry, A. Doran, M. P. Cruz, Y. H. Chu, C. Ederer, N. A. Spaldin, R. R. Das, D. M. Kim, S. H. Baek, C. B. Eom, R. Ramesh, F. Matsukura, Y. Tokura, and H. Ohno, "Electrical control of antiferromagnetic domains in multiferroic bifeo₃ films at room temperature," *Nature Materials* **5**, 823–829 (2006).
- ⁵⁶⁰ ⁹A. Roy, R. Gupta, and A. Garg, "Multiferroic memories," *Advances in Condensed Matter Physics* **2012**, 1–12 (2012).
- ⁵⁶² ¹⁰C. A. F. Vaz, "Electric field control of magnetism in multiferroic heterostructures," *Journal of Physics: Condensed Matter* **24**, 333201 (2012).
- ⁵⁶⁵ ¹¹H. Béa, M. Bibes, S. Petit, J. Kreisel, and A. Barthélémy, "Structural distortion and magnetism of bifeo₃epitaxial thin films: A raman spectroscopy and neutron diffraction study," *Philosophical Magazine Letters* **87**, 165–174 (2007).
- ⁵⁶⁹ ¹²G. Catalan and J. F. Scott, "Physics and applications of bismuth ferrite," *Advanced Materials* **21**, 2463–2485 (2009).
- ⁵⁷¹ ¹³T. F. Connolly and E. D. Copenhagen, *Bibliography of Magnetic Materials and Tabulation of Magnetic Transition Temperatures*, Vol. 5 (IFI/PLENUM, 1972).
- ⁵⁷⁴ ¹⁴W. H. Meiklejohn and C. P. Bean, "New magnetic anisotropy," *Physical Review* **102**, 1413–1414 (1956).
- ⁵⁷⁶ ¹⁵A. Misra, U. Nowak, and K. D. Usadel, "Structure of domains in an exchange-bias model," *Journal of Applied Physics* **95**, 1357–1363 (2004).
- ⁵⁷⁹ ¹⁶Z. Li and S. Zhang, "Coercive mechanisms in ferromagnetic-antiferromagnetic bilayers," *Physical Review B* **61**, R14897–R14900 (2000).
- ⁵⁸² ¹⁷C. Ederer and N. A. Spaldin, "Recent progress in first-principles studies of magnetoelectric multiferroics," *Current Opinion in Solid State and Materials Science* **9**, 128–139 (2005).
- ⁵⁸⁵ ¹⁸Y. H. Chu, L. W. Martin, Q. Zhan, P. L. Yang, M. P. Cruz, K. Lee, M. Barry, S. Y. Yang, and R. Ramesh, "Epitaxial multiferroic bifeo₃thin films: Progress and future directions," *Ferroelectrics* **354**, 167–177 (2007).
- ⁵⁸⁹ ¹⁹Y.-H. Chu, Q. He, C.-H. Yang, P. Yu, L. W. Martin, P. Shafer, R. Ramesh, F. Matsukura, Y. Tokura, and H. Ohno, "Nanoscale control of domain architectures in bifeo₃ thin films," *Nano Letters* **9**, 1726–1730 (2009).
- ⁵⁹³ ²⁰J. T. Heron, D. G. Schlom, and R. Ramesh, "Electric field control of magnetism using bifeo₃-based heterostructures," *Applied Physics Reviews* **1**, 021303 (2014).
- ⁵⁹⁶ ²¹D. Lebeugle, A. Mougin, M. Viret, D. Colson, J. Allibe, H. Béa, E. Jacquet, C. Deranlot, M. Bibes, and A. Barthélémy, "Exchange coupling with the multiferroic compound *bifeo₃* in antiferromagnetic multidomain films and single-domain crystals," *Physical Review B* **81**, 134411 (2010).
- ⁶⁰¹ ²²H. Katayama, M. Hamamoto, J. Sato, Y. Murakami, and K. Kojima, "New developments in laser-assisted magnetic recording," *IEEE Transactions on Magnetics* **36**, 195–199 (2000).
- ⁶⁰⁴ ²³S. Zhang, P. M. Levy, and A. Fert, "Mechanisms of spin-polarized current-driven magnetization switching," *Physical Review Letters* **88**, 236601 (2002).
- ⁶⁰⁷ ²⁴D. Weller and A. Moser, "Thermal effect limits in ultrahigh-density magnetic recording," *IEEE Transactions on Magnetics* **35**, 4423–4439 (1999).
- ⁶¹⁰ ²⁵L. W. Martin, Y.-H. Chu, M. B. Holcomb, M. Huijben, P. Yu, S.-J. Han, D. Lee, S. X. Wang, and R. Ramesh, "Nanoscale control of exchange bias with bifeo₃thin films," *Nano Letters* **8**, 2050–2055 (2008).
- ⁶¹³ ²⁶H. Naganuma, M. Oogane, and Y. Ando, "Exchange biases of co, py, co40fe40b20, co75fe25, and co50fe50 on epitaxial bifeo₃ films prepared by chemical solution deposition," *Journal of Applied Physics* **109** (2011), 10.1063/1.3563061.
- ⁶¹⁶ ²⁷M. C. He, B. You, H. Q. Tu, Y. Sheng, Q. Y. Xu, W. B. Rui, Y. Gao, Y. Q. Zhang, Y. B. Xu, and J. Du, "Temperature dependent exchange bias training effect in single-crystalline bifeo₃/co bilayers," *Journal of Applied Physics* **117**, 17C745 (2015).
- ⁶¹⁹ ²⁸X. Xue, X. Yuan, W. Rui, Q. Xu, B. You, W. Zhang, S. Zhou, and J. Du, "Temperature dependent exchange bias effect in polycrystalline bifeo₃/FM (FM = nife, co) bilayers," *The European Physical Journal B* **86**, 121 (2013).
- ⁶²² ²⁹S. Soeya, T. Imagawa, K. Mitsuoka, and S. Narishige, "Distribution of blocking temperature in bilayered ni81fe19/nio films," *Journal of Applied Physics* **76**, 5356 (1994).
- ⁶²⁵ ³⁰K. O'Grady, L. Fernandez-Outon, and G. Vallejo-Fernandez, "A new paradigm for exchange bias in polycrystalline thin films," *Journal of Magnetism and Magnetic Materials* **322**, 883–899 (2010).
- ⁶²⁸ ³¹T. Hauguel, S. P. Pogossian, D. T. Dekadjevi, D. Spenato, J.-P. Jay, M. V. Indenbom, and J. B. Youssef, "Experimental evidence for exchange bias in polycrystalline bifeo₃/ni₈₁fe₁₉ thin films," *Journal of Applied Physics* **110**, 073906 (2011).
- ⁶³¹ ³²T. Hauguel, S. P. Pogossian, D. T. Dekadjevi, D. Spenato, J.-P. Jay, and J. Ben Youssef, "Driving mechanism of exchange bias and magnetic anisotropy in multiferroic polycrystalline bifeo₃/permalloy bilayers," *Journal of Applied Physics* **112**, 093904 (2012).
- ⁶³⁴ ³³V. Baltz, B. Rodmacq, A. Zarefy, L. Lechevallier, and B. Dieny, "Bimodal distribution of blocking temperature in exchange-biased ferromagnetic/antiferromagnetic bilayers," *Physical Review B* **81**, 52404 (2010).
- ⁶³⁷ ³⁴C. K. Safeer, M. Chamfrault, J. Allibe, C. Carretero, C. Deranlot, E. Jacquet, J.-F. Jacquot, M. Bibes, A. Barthélémy, B. Dieny, H. Béa, and V. Baltz, "Anisotropic bimodal distribution of blocking temperature with multiferroic bifeo₃ epitaxial thin films," *Applied Physics Letters* **100**, 2402 (2012).
- ⁶⁴⁰ ³⁵J. Ventura, J. P. Araujo, J. B. Sousa, A. Veloso, and P. P. Freitas, "Distribution of blocking temperatures in nano-oxide layers of specular spin valves," *Journal of Applied Physics* **101**, 113901–113901 (2007).
- ⁶⁴³ ³⁶J. Nogués, J. Sort, V. Langlais, V. Skumryev, S. Suriñach, J. S. Muñoz, and M. D. Baró, "Exchange bias in nanostructures," *Physics Reports* **422**, 65–117 (2005).
- ⁶⁴⁶ ³⁷M. Li, Y.-P. Zhao, G.-C. Wang, and H.-G. Min, "Effect of surface roughness on magnetization reversal of co films on plasma-etched si(100) substrates," *Journal of Applied Physics* **83**, 6287–6289 (1998).
- ⁶⁴⁹ ³⁸S. S. Rao, J. T. Prater, F. Wu, C. T. Shelton, J.-P. Maria, and J. Narayan, "Interface magnetism in epitaxial bifeo₃/la0.7sr0.3mno3heterostructures integrated on si(100)," *Nano Letters* **13**, 5814–5821 (2013).
- ⁶⁵² ³⁹C. Ederer and N. A. Spaldin, "Weak ferromagnetism and magnetoelectric coupling in bismuth ferrite," *Physical Review B* **71**,

- 668 60401 (2005).
- 669 ⁴⁰C. Ederer and C. J. Fennie, "Electric-field switchable magne- 703
670 tization via the dzyaloshinskii moriya interaction: *Fetio₃* ver- 704
671 sus *bifeo₃*," Journal of Physics: Condensed Matter **20**, 434219 705
672 (2008).
- 673 ⁴¹H. Naganuma, A. Kovacs, A. Hirata, Y. Hirotsu, and S. Oka- 706
674 mura, "Structural analysis of polycrystalline *bifeo₃* films by 707
675 transmission electron microscopy," MATERIALS TRANSAC- 708
676 TIONS **48**, 2370–2373 (2007).
- 677 ⁴²I. O. Troyanchuk, M. V. Bushinsky, A. N. Chobot, O. S. Man- 709
678 tytskaya, and N. V. Tereshko, "Weak ferromagnetism in *bifeo₃*- 710
679 based multiferroics," JETP Letters **89**, 180–184 (2009).
- 680 ⁴³M. Ramazanoglu, M. Laver, W. Ratcliff, S. M. Watson, W. C. 711
681 Chen, A. Jackson, K. Kothapalli, S. Lee, S.-W. Cheong, and 712
682 V. Kiryukhin, "Local weak ferromagnetism in single-crystalline 713
683 ferroelectric *bifeo₃*," Physical review letters **107**, 207206 (2011).
- 684 ⁴⁴B. Marchand, P. Jalkanen, V. Tuboltsev, M. Vehkamäki, M. Put- 714
685 taswamy, M. Kemell, K. Mizohata, T. Hatanpää, A. Savin, 715
686 J. Räisänen, M. Ritala, and M. Leskelä, "Electric and magnetic 716
687 properties of ALD-grown *bifeo₃*films," The Journal of Physical 717
688 Chemistry C **120**, 7313–7322 (2016).
- 689 ⁴⁵J. C. Slonczewski, "Fluctuation mechanism for biquadratic ex- 718
690 change coupling in magnetic multilayers," Physical Review Let- 719
691 ters **67**, 3172–3175 (1991).
- 692 ⁴⁶N. C. Koon, "Calculations of exchange bias in thin films with fer- 720
693 romagnetic/antiferromagnetic interfaces," Physical Review Let- 721
694 ters **78**, 4865–4868 (1997).
- 695 ⁴⁷J.-G. Hu, G. Jin, A. Hu, and Y.-Q. Ma, "Temperature 722
696 dependence of exchange bias and coercivity in ferromag- 723
697 netic/antiferromagnetic bilayers," The European Physical Jour- 724
698 nal B - Condensed Matter and Complex Systems **40**, 265 (2004).
- 699 ⁴⁸T. J. Moran, J. Nogués, D. Lederman, and I. K. Schuller, "Per- 725
700 pendicular coupling at FeFeF₂ interfaces," Applied Physics Let- 726
701 ters **72**, 617 (1998).
- 702 ⁴⁹M. Dumm, M. Zölfli, R. Moosbühler, M. Brockmann, T. Schmidt, 727
703 and G. Bayreuther, "Magnetism of ultrathin feco (001) films on 728
704 gaas(001)," Journal of Applied Physics **87**, 5457 (2000).
- 705 ⁵⁰R. P. Michel, A. Chaiken, C. T. Wang, and L. E. Johnson, 729
706 "Exchange anisotropy in epitaxial and polycrystalline nio/nfe 730
707 bilayers," Physical Review B **58**, 8566–8573 (1998).
- 708 ⁵¹J. McCord and R. Schäfer, "Domain wall asymmetries in 731
709 ni81fe19/nio: proof of variable anisotropies in exchange bias sys- 732
710 tems," New Journal of Physics **11**, 083016 (2009).
- 711 ⁵²J. McCord, C. Hamann, R. Schäfer, L. Schultz, and R. Mattheis, 733
712 "Nonlinear exchange coupling and magnetic domain asymmetry 734
713 in ferromagnetic/irmn thin films," Physical Review B **78**, 094419 735
714 (2008).
- 715 ⁵³D. T. Dekadjevi, T. Jaouen, D. Spenato, S. P. Pogossian, and 736
716 J. Ben Youssef, "Experimental evidences and driving mechanisms 737
717 for anisotropic misalignments in exchange coupled systems," The 738
718 European Physical Journal B **80**, 121–125 (2011).
- 719 ⁵⁴D. Spenato, V. Castel, S. P. Pogossian, D. T. Dekadjevi, and 739
720 J. Ben Youssef, "Asymmetric magnetization reversal behavior in 740
721 exchange-biased nife/mnpt bilayers in two different anisotropy 741
722 regimes: Close and far from critical thickness," Applied Physics 742
723 Letters **91**, 062515 (2007).
- 724 ⁵⁵J.-g. Hu, G.-j. Jin, and Y.-q. Ma, "Thickness and angular de- 743
725 pendencies of exchange bias in ferromagnetic/antiferromagnetic 744
726 bilayers," Journal of Applied Physics **92**, 1009 (2002).
- 727 ⁵⁶E. Jiménez, J. Camarero, J. Sort, J. Nogués, A. Hoffmann, F. J. 745
728 Teran, P. Perna, J. M. García-Martín, B. Dieny, and R. Mi- 746
729 randa, "Highly asymmetric magnetic behavior in exchange biased 747
730 systems induced by noncollinear field cooling," Applied Physics 748
731 Letters **95**, 122508 (2009); E. Jiménez, J. Camarero, P. Perna, 749
732 N. Mikuszeit, F. J. Terán, J. Sort, J. Nogués, J. M. García- 750
733 Martín, A. Hoffmann, B. Dieny, and R. Miranda, "Role of 751
734 anisotropy configuration in exchange-biased systems," Journal of 752
735 Applied Physics **109**, 07D730 (2011).
- 736 ⁵⁷J. D. Hunter, "Matplotlib: A 2d graphics environment," Com- 753
737 putting in Science & Engineering **9**, 90–95 (2007).